

# Development of a Mathematical Model of the Human Circulatory System

MARTIN J. CONLON,<sup>1</sup> DONALD L. RUSSELL,<sup>1</sup> and TOFY MUSSIVAND<sup>2</sup>

<sup>1</sup>Department of Mechanical and Aerospace Engineering, Carleton University, 1125 Colonel By Drive, Ottawa, ON, Canada K1S 5B6 and <sup>2</sup>University of Ottawa Heart Institute, 40 Ruskin Street, Ottawa, ON, Canada K1Y 4W7

(Received 19 October 2004; accepted 12 July 2006; published online: 9 August 2006)

**Abstract**— A mathematical lumped parameter model of the human circulatory system (HCS) has been developed to complement *in vitro* testing of ventricular assist devices. Components included in this model represent the major parts of the systemic HCS loop, with all component parameters based on physiological data available in the literature. Two model configurations are presented in this paper, the first featuring elements with purely linear constitutive relations, and the second featuring nonlinear constitutive relations for the larger vessels. Three different aortic compliance functions are presented, and a pressure-dependent venous flow resistance is used to simulate venous collapse. The mathematical model produces reasonable systemic pressure and flow behaviour, and graphs of this data are included.

**Keywords**—Cardiovascular system model, Mathematical model, Human circulatory system.

## NOMENCLATURE

$\mu$	viscosity, $\text{kg cm}^{-1} \text{s}^{-1}$
$\Phi_C$	vessel compliance function
$\Phi_I$	vessel inertance function
$\Phi_R$	vessel resistance function
$\rho$	density, $\text{kg cm}^{-3}$
$A$	cross-sectional area, $\text{cm}^2$
$C$	compliance, $\text{cm}^5 \text{N}^{-1}$
$D$	diameter, cm
$F$	pumping force, N
$I$	fluid inertance, $\text{N s}^2 \text{cm}^{-5}$
$I_{\text{ht}}$	heart pumping plate mass, $\text{N s}^2 \text{cm}^{-1}$
$L$	length, cm
$P$	pressure, $\text{N cm}^{-2}$
$p$	fluid momentum, $\text{N s cm}^{-2}$
$p_{\text{ht}}$	heart pumping plate momentum, N s
$Q$	volume flow rate, $\text{cm}^3 \text{s}^{-1}$
$R$	radius, cm or flow resistance, $\text{N s cm}^{-5}$
$R_{\text{ht}}$	friction in the pump, $\text{N s cm}^{-1}$
$r$	radial position coordinate, cm

$s_{\text{ht}}$	heart pumping plate position, cm
$u$	velocity, $\text{cm s}^{-1}$
$V$	volume, $\text{cm}^3$
$x$	linear position coordinate, cm
$\square_a$	subscript refers to artery (SCM)
$\square_{\text{ao}}$	subscript refers to aorta (DCM)
$\square_{\text{at}}$	subscript refers to arteries (DCM)
$\square_{\text{ht}}$	subscript refers to heart (pump)
$\square_{\text{incn}}$	subscript refers to inlet cannula
$\square_{\text{inv}}$	subscript refers to inlet valve
$\square_{\text{otcn}}$	subscript refers to outlet cannula
$\square_{\text{otv}}$	subscript refers to outlet valve
$\square_{\text{pe}}$	subscript refers to peripheral system
$\square_v$	subscript refers to venous system (SCM)
$\square_{\text{vc}}$	subscript refers to vena cava (DCM)
$\square_{\text{vn}}$	subscript refers to venous system (DCM)

## INTRODUCTION

Much total artificial heart (TAH) and left ventricular assist device (LVAD) development work is performed *in vitro*, using so-called “mock circulatory systems.” The mock circulatory system (MCS) provides short- and long-term performance and reliability data, which is key to the development process, however most MCS configurations allow for limited study of the actual circulation blood flow dynamics. A mathematical model of the human circulatory system (or even the MCS) complements this *in vitro* testing, as it permits the study of features and behaviours that would be impractical to investigate using a physical mock circulatory system. For example, model components can be added or removed, and their parameters varied with relative ease. Results for a wide range of situations can be found quickly by simulation thus identifying areas for productive experimental study.

This paper presents a mathematical lumped parameter model of the human circulatory system (HCS). As this mathematical model is geared towards LVAD development, the pulmonary loop is not included, although it could be added later. The components included in the model

Address correspondence to Donald L. Russell, Department of Mechanical and Aerospace Engineering, Carleton University, 1125 Colonel By Drive, Ottawa, ON, Canada K1S 5B6. Electronic mail: drussell@mae.carleton.ca

represent the major parts of the systemic HCS loop, with constitutive parameters selected based on values found in the literature. Correlations between this model and several MCS configurations can also be made, providing an alternate means of validating the model. Validation of the model using human test data is more problematic, with suitable *in vivo* data being difficult to obtain.

Our model resolves the systemic side of the human circulatory system with a moderate level of detail; all parameters are based on human physiological data available in the literature. Other models<sup>12</sup> treat the system in more detail, but are often based on the more extensive non-human physiological, published data (such as porcine or canine data, the latter being the case for Lu). There are also simpler models such as Xu<sup>27</sup> or Lee<sup>10</sup> which either treat the system with a coarser level of detail or focus on a single subsystem such as the arterial system. All published human circulatory models are aimed at accurately studying specific features of the circulatory system (e.g., baroreceptor response). Our model is focused on the dynamic interaction between a cardiovascular support device and the systemic circulation.

The hydraulic basis of our model also presents an advantage over the electrical analogues of the HCS which are prevalent in the literature, such as Xu<sup>27</sup> or Lee,<sup>10</sup> because the flow loops are realistic; electrical analogues require non-physical connections to ensure proper grounding.<sup>24</sup>

It should be noted that studying or modelling the systemic circulation at anything other than a macro level is futile because all of the parameters change from person to person, and indeed continuously within the same person. The goal of this work is to study the large scale flow characteristics within the human circulatory system, enabling us to predict pressures and flow rates within the body. The segment parameters in the model may be varied dynamically, but there is no guidance or basis for this.

## HYDRAULICS

In this work, all the vessels in the human circulatory system are treated as smooth, thin-walled, flexible tubes. Blood flow in the circulatory system is assumed laminar, and has a low Reynold's Number, normally taken between 2000–5000.<sup>5</sup> The vessel cross-sectional diameter is approximated as constant under the assumption that all vessel expansion occurs axially. In this initial model the effects of gravity are ignored as in the case where the “patient” is lying down. Note that the derivations in this section are valid for any consistent set of units.

The expansion or contraction of the vessels can be considered equivalent to a change in blood density within our engineering control volume (the blood vessel). Under our assumption that there is no difference in elevation between the inflow and outflow ends of the control volume, this term vanishes from the continuity equation.<sup>25</sup> Note that modelling vessel diameter changes in this way is not straightfor-

ward from an energetic view point and, if included, would need to be carefully handled with our modelling approach, the energy-based bond graph method.

Blood vessels can be idealized as cylindrical tubes. If we assume no swirl flow, or circumferential variation in velocity, and the flow is fully developed (the fluid velocity at a given radial distance does not change along the length of the vessel), the exact solution for fully developed flow in a horizontal vessel is given by the Hagen-Poiseuille<sup>25</sup> equation:

$$\begin{aligned} Q &= \int u dA \\ &= \int_0^R u_{\max} \left(1 - \frac{r^2}{R^2}\right) 2\pi r dr \\ &= \frac{\pi R^4}{8\mu} \left(-\frac{dP}{dx}\right) \end{aligned} \quad (1)$$

From an energetic point of view, a vessel's flow resistance,  $\Phi_R$ , specifies the pressure drop across the segment as a function of flow rate:

$$\begin{aligned} \Delta P(Q) &= \Phi_R(Q) \\ &= \frac{8\mu}{\pi R^4} \cdot L \cdot Q \\ &= \frac{128\mu}{\pi D^4} \cdot L \cdot Q \end{aligned} \quad (2)$$

The flow inertia,  $\Phi_I$ , in a segment of vessel describes the relationship between the fluid's momentum and flow rate:

$$\begin{aligned} p(Q) &= \Phi_I(Q) \\ &= \frac{\rho \cdot L}{A} Q \end{aligned} \quad (3)$$

Similarly, a vessel's compliance ( $\Phi_C$ , which is the inverse of stiffness) defines the change in internal volume for a given change in internal pressure:

$$\begin{aligned} V(P) &= \Phi_C(P) \\ &= C \cdot P \end{aligned} \quad (4)$$

Each of these parameters must be determined for a given lumped segment of vessel. Unfortunately, obtaining good physiological data is difficult; most studies of vessel properties are performed *in vitro*, using tissue from cadavers, and the parameters of interest change postmortem, making characterisation difficult. In spite of this, there is physiological data in the literature, and these data were used as an aid in tuning the model.

**TABLE 1. Properties of vessels in the circulatory system.**<sup>5,22,23</sup>

	Aorta	Arteries	Arterioles	Capillaries	Venules	Veins	Venae Cavae
Diameter (cm)	2.5	0.4	0.003	0.0008	0.002	0.5	3.0
Length (cm)	20	30	—	30	—	30	50
Velocity (cm s <sup>-1</sup> )	40	10–50	0.1	0.03	0.3	0.3–5	5–20
Volume (L)	0.15	0.65	0.15	0.2	0.15	2.55	0.5
Pressure (mm Hg)	80–120	40–110	25–40	10–25	8–12	4–10	2–5
Compliance (cm <sup>5</sup> N <sup>-1</sup> )	28	81	75	100	280	3800	1300
Resistance (N s cm <sup>-5</sup> )	0.0053	0.0013	0.0036	0.0027	0.0012	0.00032	0.0004
Inertance (N s <sup>2</sup> cm <sup>-5</sup> )	$2.4 \times 10^{-4}$	$1.5 \times 10^{-5}$	—	$1.2 \times 10^{-7}$	—	$3.8 \times 10^{-6}$	$6.3 \times 10^{-5}$

## MODEL

The circulatory system model<sup>21</sup> was segmented into the arterial system, the peripheral system (subsuming the arterioles, venioles and capillaries) and the venous system. The LVAD model (featuring a simple piston and compliant blood sac configuration) was connected to the circulatory system model using two cannulae. Inlet and outlet valves were passive-type, with an adjustable offset pressure. (In this work the bias or offset pressure was set to zero.)

This basic model was refined by segmenting the arterial system into aortic- and artery-segments to study the effects of nonlinearities on the arterial pressure and flow waveforms,<sup>14</sup> and the venous system into small- and large-veins to study the effects of vena cava collapse under low internal pressures (or applied suction).<sup>2</sup>

Estimates of the various vessel properties (such as cross sectional area, and length) are available in the literature. Table 1 summarizes some of these from a variety of sources.<sup>5,22,23</sup>

The various subunits will now be described in greater detail, beginning with the LVAD, and following the circulation back to the heart.

### LVAD (Pump)

In this simulation, the blood is motivated by a simple pump, referred to throughout this work as an LVAD (or “the LVAD”). This pump is a simple piston-cylinder configuration with a compliant blood sac and is not based on any current VAD design. It features two passive flow valves which open or close based on the pressure gradient across the valve. Operating in “full-fill, full-eject” mode, the pump cycle (ejection and filling) functions as follows:

- At the onset of ejection, a constant, positive force is applied to the piston, increasing the internal pressure in the compliant blood chamber.
- The increase in internal pressure results in the closure of the inlet valve and opening of the outlet

valve. Note that the valves are passive, and therefore do not necessarily open or close at the same instant.

- Blood is expelled from the pump (ejection) through the outlet valve until the internal blood volume reaches a preset minimum level (“full eject”), signalling the end of the ejection phase, and the beginning of filling.
- The piston force is reduced for LVAD filling; this lowers the internal blood sac pressure, and reverses the pressure gradients across the two valves. The outlet valve closes and the inlet valve opens. (Again, not necessarily at the same time.)
- The piston regresses to its original position as blood flows into the pump (filling), and once the blood volume reaches a preset maximum level (the “full-fill” condition) the cycle repeats.

The pump can also operate in a “fixed rate” mode, with preset time intervals for ejection and filling. In this case the pump would function as follows:

- At the onset of ejection, a constant, positive force is applied to the piston, increasing the internal pressure in the compliant blood chamber.
- The increase in internal pressure results in the closure of the inlet valve and opening of the outlet valve. As above, the valves are passive, and therefore do not necessarily open or close at the same instant.
- Blood is expelled from the pump (ejection) through the outlet valve for a fixed length of time. The ratio of this time to the total cycle length is referred to as the “ejection duty cycle.”
- The piston force is reduced for LVAD filling; this lowers the internal blood sac pressure, and reverses the pressure gradients across the two valves. The outlet valve closes and the inlet valve opens. (Again, not necessarily at the same time.)
- The piston regresses as blood flows into the pump (filling) for a fixed length of time.

### Cannulae

The pump connects to the HCS via two cannulae, modelled as thin, flexible tubes with limited compliance. Both cannulae were assumed to have the same internal diameter of 2.0 cm (which is reasonable for this type of cannula), and the lengths were chosen as 15 cm and 10 cm for the outlet and inlet cannula (respectively). The term “outlet cannula” refers to the cannula attached to the outflow side of the LVAD.

Compliances for the two cannulae are based on results from Ogino *et al.*<sup>16</sup> who measured the compliance of cannulae made of several materials. We have chosen to base our values on their reported compliance of  $0.0129 \text{ cm}^3 \text{ mm Hg}^{-1}$  that corresponds to a “soft” cannula with a length of 115 mm, tapering from a diameter of 22 mm to a diameter of 18 mm. Scaling this value to the lengths used in the model, the compliance of the output cannula is  $0.79 \text{ N cm}^{-5}$  and the compliance of the input cannula is  $1.19 \text{ N cm}^{-5}$ .

The flow inertances for the two cannulae were computed using the standard hydraulic equation for smooth tubes found in Section 2. The flow inertance for the outlet cannula is  $5.1 \times 10^{-5} \text{ N s}^2 \text{ cm}^{-5}$ , and for the inlet cannula is  $3.41 \times 10^{-5} \text{ N s}^2 \text{ cm}^{-5}$ . The inlet cannula resistance was calculated using Eq. (3) with a blood density of  $1.07 \text{ g cm}^{-3}$ :

$$\Delta P_{\text{incn}}(Q) = 1.3 \times 10^{-5} Q \quad [\text{N cm}^{-2}] \quad (5)$$

The resistance of the outlet cannula is difficult to calculate using basic hydraulic equations due to the complex nature of the flow. Instead it is based on adjusting the value to generate appropriate responses in the system. The value used is consistent with other similar values found in the

literature (for example the aortic resistance used in<sup>1</sup>):

$$\Delta P_{\text{otcn}}(Q) = 0.0011 Q \quad [\text{N cm}^{-2}] \quad (6)$$

### Valves

Flow in-to and out-of the pump is controlled by passive valves. The flow resistance through a valve depends on the valve state (open or closed), determined by the pressure gradient across the valve. Flow resistance through the valve was set at  $8 \times 10^{-4} \text{ N s cm}^{-5}$  when the valve was open, and  $8 \times 10^2 \text{ N s cm}^{-5}$  when the valve was closed.

### Arteries (and Aorta)

The pressure-volume relationship for the larger arterial vessels is nonlinear, but these nonlinearities can be neglected for a first approximation, and the entire arterial system treated as a single compliance. This is what is found in the Donovan MCS<sup>3</sup> and many other MCSs.<sup>8,20,26</sup> Studies<sup>11</sup> comparing linear and nonlinear models of the arterial system have shown that a linear element tends to underestimate the end-diastolic pressure (which corresponds to the lowest arterial pressure during heart filling) and overestimate the peak systolic pressure (which corresponds to the maximum arterial pressure during ejection). The linear compliance model tends to behave well only about the mean arterial pressure; when the volume of blood is outside the nominal range, the pressures predicted by the linear model correlate poorly with those observed in the body.

Nevertheless, the entire arterial system (including the aorta) can be modelled as in the top half of Fig. 1, using a single compliance element.<sup>21</sup> The constitutive relationship of this element relates the volume of the arterial system to changes in internal pressure. In the preliminary model,

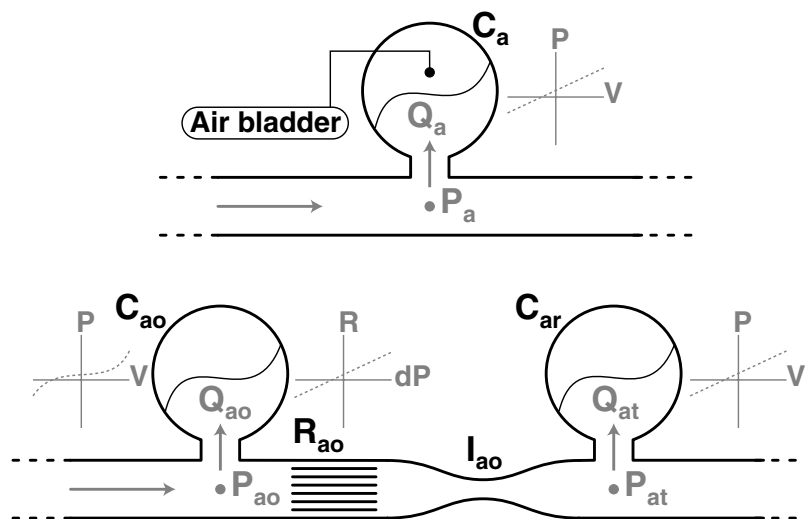


FIGURE 1. Two arterial system models.

the compliance was assumed to be constant at a value of  $100 \text{ cm}^5 \text{ N}^{-1}$  as per the results presented in Laskey,<sup>9</sup> which studied arterial pressure in ten patients. (That particular study found a mean compliance of  $100 \text{ cm}^5 \text{ N}^{-1}$  with a standard deviation of  $2 \text{ cm}^5 \text{ N}^{-1}$ ). This value was later changed to  $130 \text{ cm}^5 \text{ N}^{-1}$ , to reflect newer data appearing in the literature.<sup>18</sup> The pressure at nominal volume was chosen as  $1.33 \text{ N cm}^{-2}$  ( $100 \text{ mm Hg}$ ) to match the pressures in the human arterial system<sup>5</sup> and the nominal volume was chosen as  $700 \text{ cm}^3$ . This gives the following constitutive relation:

$$P_a(V) = \frac{V}{130} - 4.05 \quad [\text{N cm}^{-2}] \quad (7)$$

A more refined version of the arterial model was subsequently developed.<sup>14</sup> This configuration, the so-called dual-compliance model (DCM), is illustrated in the bottom half of Fig. 1 and consists of two compliance elements coupled with an inertial element. Once again this model was based on physiological data. There are studies showing the pressure-volume characteristics of the human aorta.<sup>7,11</sup> The aortic compliance in the dual-compliance model was chosen to match data from the age group of 47–52 years given in King.<sup>7</sup> The data used by King were obtained during dissection of a human cadaver. Although tissue properties change post-mortem, this data was assumed to apply *in vivo* and was used because no *in vivo* source of data was available. Tissues tend to lose their internal residual stress and elongation of the segment is possible unless careful experimental procedures are followed.

Three separate curves were fitted to the experimental data, by minimizing the error (in the least squares sense) between the function(s) and the data points. These curve fits (and the data points) are plotted in Fig. 2. The linear fit gave an aortic compliance of  $29.3 \text{ cm}^5 \text{ N}^{-1}$ , with an offset of  $-1.94 \text{ N cm}^{-2}$ :

$$P_{ao}|_{\text{lin}} = \frac{V}{29.3} - 1.94 \quad [\text{N cm}^{-2}] \quad (8)$$

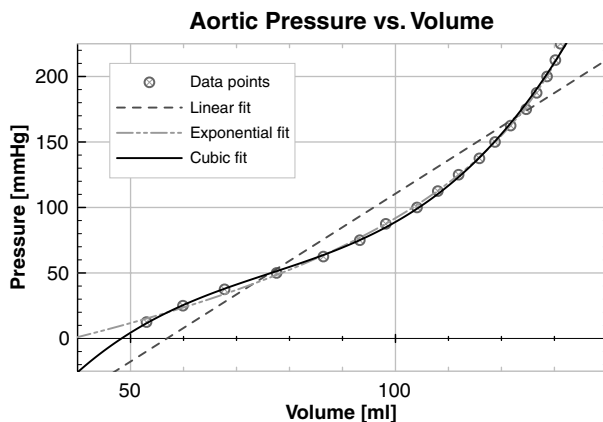


FIGURE 2. Aortic pressure-volume data and curve fits.

The cubic aortic compliance function is:

$$P_{ao}|_{\text{cub}} = 7.66 \times 10^{-6} \cdot V^3 - 0.00175 \cdot V^2 + 0.151 \cdot V - 4.08 \quad [\text{N cm}^{-2}] \quad (9)$$

The exponential aortic compliance function is:

$$P_{ao}|_{\text{exp}} = -1.43 \cdot \ln(1.37 - 0.00943 \cdot V) \quad [\text{N cm}^{-2}] \quad (10)$$

In the dual-compliance model, the arterial compliance is dependent on the aortic compliance. The value of aortic compliance obtained by the linear least-squares fit ( $29.3 \text{ cm}^5 \text{ N}^{-1}$ ) is subtracted from the total systemic arterial compliance of  $130 \text{ cm}^5 \text{ N}^{-1}$  to give an arterial compliance of  $101 \text{ cm}^5 \text{ N}^{-1}$ , and the pressure at nominal volume is again taken to be  $1.33 \text{ N cm}^{-2}$ .

$$P_{at}(V) = \frac{V}{101} - 4.64 \quad [\text{N cm}^{-2}] \quad (11)$$

This ensures that the single- and dual-compliance systemic arterial models behave similarly when inserted in the overall HCS model.

The dual-compliance model was initially simulated without a flow resistance element in order to study the pressure oscillations which are produced due to the presence of the two compliances. These oscillations override the nominal pressure behaviour, changing the shape of the curve and distorting the maximum and minimum pressures in the aorta. This behaviour is undesirable, and the aortic resistance element was tuned to provide a smooth pressure waveform, and a more accurate flow rate waveform shape (as compared with the initial, single-compliance model). These improvements will be further discussed in the “Simulation Results” section.

The required flow resistance of  $0.0011 \text{ N s cm}^{-5}$  is substantially larger than the resistance which would be computed based on Eq. (2) (with an aortic diameter of  $2.5 \text{ cm}$ , and length of  $20 \text{ cm}$ <sup>22</sup> the expected flow resistance would be  $2.09 \times 10^{-6} \text{ N s cm}^{-5}$ ). The higher resistance in the aorta was chosen so that the performance of the simulations was acceptable. The larger value may reflect effects of unsteady flow, changing flow geometry and losses from the stretching and relaxing of the vessel walls and is consistent with the literature (see for example<sup>1</sup>).

Blood flow in the vessels proximal to the LVAD (the outflow cannula, and possibly the aorta) will likely be turbulent, as opposed to laminar; turbulent flow results in larger pressure losses, which would also justify the larger aortic resistance element.

Simulation of the aortic segment with the selected flow resistance yields pressure and flow behaviour similar to

that found in the human circulatory system. Once again, these details will be presented in the “Simulation Results” section.

The dual-compliance model includes an inertance element to dynamically decouple the states for the aortic and arterial segments. The inertance allows the volume in the aorta and the volume in the arterial segment (which excludes the aorta in the dual-compliance model) to vary independently. The value of inertance was calculated using Eq. (3) based on the typical length and cross-sectional area estimates for the aorta. As above, the diameter was taken as 2.5 cm and the length as 20 cm (generally accepted values for the average diameter and length of the larger arterial vessels). Values of aortic inertance can vary from individual to individual. The aortic inertance that can be estimated based on Eq. (3) (using a blood density of  $1.07 \text{ g cm}^{-3}$ ) is  $4.36 \times 10^{-5} \text{ N s}^2 \text{ cm}^{-5}$  which generally agrees with the values published in the literature.<sup>5</sup> This value is used in the simulations.

#### *Peripheral Circulation*

The peripheral circulation model consists of an inertance element and a flow resistance element, representing all of the micro circulation in the body. The capillaries and the venules (which would be counted as part of the peripheral circulatory system) have an extremely small cross-sectional area, but a very large total cross-sectional area, meaning that they have a large flow inertia and significant flow resistance, but very small stiffness.

The peripheral flow inertance and resistance parameters are not directly available in the literature, because these individual lumps model a complex, continuous system of vessels. The selected parameters were based on data from Tortora,<sup>22</sup> Fung,<sup>5</sup> Guyton<sup>6</sup> and Tsach *et al.*<sup>23</sup> giving a peripheral flow inertance of  $0.0275 \text{ N s}^2 \text{ cm}^{-5}$  and a peripheral flow resistance of  $0.013 \text{ N s cm}^{-5}$ .

#### *Venous Segment*

As with the aorta and arteries, the larger veins in the body such as the various venae cavae can be modelled as thin-walled, flexible tubes. As such their pressure-volume constitutive relations are again nonlinear, but these nonlinear effects can be ignored for a first approximation. To obtain results that are more accurate, especially at off-nominal conditions, these nonlinearities must be taken into account.

The most important nonlinear venous behaviour, from a modelling perspective, is the tendency towards collapse at low internal pressures. The collapse of the larger veins (as with any thin-walled tube) dramatically increases resistance to blood flow. The venous system normally operates at low internal pressures (2–5 mm Hg) and it is important to allow for the possibility of venous collapse, especially when modelling an implanted total artificial heart which is

able to apply suction to the venous system. In addition, the absence of the pulmonary loop in our model necessitates a direct connection between the LVAD model and the venous system.

The venous system is responsible for the return of blood to the heart. It consists of a series of blood vessels with increasingly larger diameters, namely the venules, the veins and the superior- and inferior-venae cavae. The venules are similar to the capillaries in that they are microscopic vessels, but unlike the capillaries, which branch off from the arteries, the venules join to return deoxygenated blood from the cells to the veins. Recall that the venules, like the capillaries, are included in the “peripheral circulation” lumped model. The veins are larger in diameter than the venules, but their mean cross-sectional area is still quite small, and collapse of the veins is not a problem. In addition, the layers of elastic fibers, smooth muscle, and outer fibrous tissue mean that the veins are not thin-walled tubes (in the engineering sense). The total cross-sectional area for the veins is quite large ( $80 \text{ cm}^2$ )<sup>5</sup> and nonlinearities in the pressure-volume relationship are negligible.

The venae cavae, on the other hand, are larger in diameter and qualify as thin-walled tubes. The average cross-sectional area is  $7 \text{ cm}^2$ .<sup>5</sup> and nonlinear behaviour at both high and low internal pressures should be taken into consideration.

For a first approximation, the entire venous system can be modelled using a single compliance element whose constitutive relation is the volume response of the venous system to changes in internal pressure, as illustrated in the top half of Fig. 3. The compliance of the element was assumed to be constant at  $3750 \text{ cm}^2 \text{ N}^{-1}$  and the pressure at nominal volume (i.e.,  $2500 \text{ cm}^3$ ) was chosen as 20 mm Hg. This pressure is slightly higher than would be found in the literature,<sup>5,22</sup> but is necessary because in this HCS model, the venous pressure is solely responsible for filling the LVAD. The LVAD requires a pressure of 5 to 15 mm Hg (normally provided by the natural heart) in order to fill, while the typical venous pressure is only 5 mm Hg. Decreasing the peripheral flow resistance in the systemic model results in a lower pressure drop across the segment, a higher average venous pressure, and sufficient filling pressure for the LVAD. Other pressures and flow rates are not affected.

The venous system model was further refined. The resultant dual-compliance model, illustrated in the bottom half of Fig. 3, is based on the realization (mentioned above) that due to the small individual diameters and large total cross-sectional area, nonlinear effects will be negligible in many of the smaller vessels in the venous system. (Specifically, the “intermediate” veins with less elastic fiber in their medial and external layers). Only the larger venae cavae, which contain a relatively small percentage of the total venous blood volume, will exhibit noticeable nonlinearities.

The venous blood volume was divided between the two compliance elements, with the first, linear, compliance

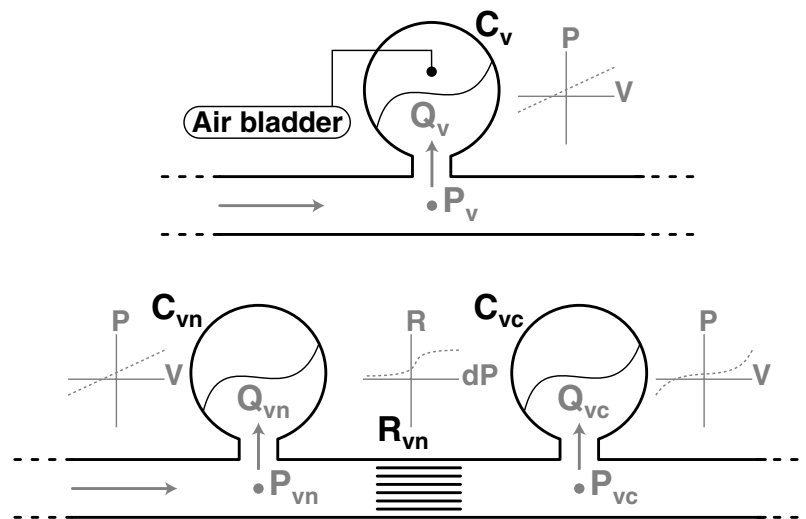


FIGURE 3. Two venous system models.

containing (nominally) 2000 cm<sup>3</sup> of the system's blood volume, and the second collapsing, nonlinear, compliance containing 600 cm<sup>3</sup> of the system's blood volume. These volumes were determined based on the overall blood volume in our model and the approximate distribution of blood between the veins and venae cavae shown in Table 1.

Splitting the venous system into two separate compliance elements has an added advantage: by inserting a nonlinear resistance element in between the two venous compliance elements, we can model the collapse of the larger veins at low internal pressures, and the corresponding increase in flow resistance. The constitutive relations for all three of these elements are inter-related. The linear compliance element is similar to that found in the single-compliance venous model. The pressure at nominal volume was chosen as 0.27 N cm<sup>-2</sup> (20 mm Hg). The venous compliance was set to 2500 cm<sup>5</sup> N<sup>-1</sup>, which results in the following constitutive relation:

$$P_{vn}(V) = \frac{V}{2500} - 0.53 \quad [\text{N cm}^{-2}] \quad (12)$$

A piecewise linear curve (with three segments) was used to model the nonlinear vena cava compliance. Below a critical volume of 500 cm<sup>3</sup> the vessel is deemed to have collapsed. The pressure at this critical volume was set to 0 N cm<sup>-2</sup> (0 mm Hg). In the nominal range of volumes from 500 cm<sup>3</sup> to 600 cm<sup>3</sup> the vena cava compliance was set to 500 cm<sup>5</sup> N<sup>-1</sup> while at volumes below 500 cm<sup>3</sup> and above 600 cm<sup>3</sup> the compliance was 0.1 cm<sup>5</sup> N<sup>-1</sup>. The pressure at the nominal vena cava volume of 600 cm<sup>3</sup> is 0.2 N cm<sup>-2</sup> (15 mm Hg) which is (again) slightly higher than that commonly found in the literature.

The resistance function was chosen to allow a flow rate of 10 cm<sup>3</sup> s<sup>-1</sup> when the vessel was collapsed, and 650 cm<sup>3</sup> s<sup>-1</sup>

when it was fully open (given a nominal pressure drop of 0.067 N cm<sup>-2</sup>). The offset, or transition pressure difference, was chosen as 0.4 N cm<sup>-2</sup> based on the two compliance functions.

The flow resistance is a function of the pressure difference between the linear venous segment and the nonlinear vena cava segment. This has the effect of increasing venous flow resistance when the vena cava internal volume drops below the critical level of 500 cm<sup>3</sup> described above.

The ability of the veins to collapse is not as important in LVAD simulation, because the LVAD is isolated from the venous system by both the pulmonary loop and the natural heart. The feature becomes more important with TAH simulation, because those devices and the venous system are connected directly. Of course an LVAD's "venous isolation" assumes the smaller, peripheral vessels provide sufficient dynamic decoupling between the arterial and venous systems. This is likely the case; as noted earlier, the peripheral vessels have extremely small individual diameters, but a very large total cross-sectional area. However, this has not been studied, and there may be something an LVAD can do to cause a specific change in the arterial system, and induce venous collapse.

### Overall Model

A hydraulic schematic of the overall circulatory system model is illustrated in Fig. 4. The major components are highlighted with grey boxes, and labelled accordingly. The arterial and venous models included in the circuit are the dual compliance models, with the corresponding single compliance models placed beside their respective dual-compliance model. Either arterial "lump" from Fig. 1 can be inserted as the Arterial System and either venous model illustrated in Fig. 3 can be inserted as the Venous System

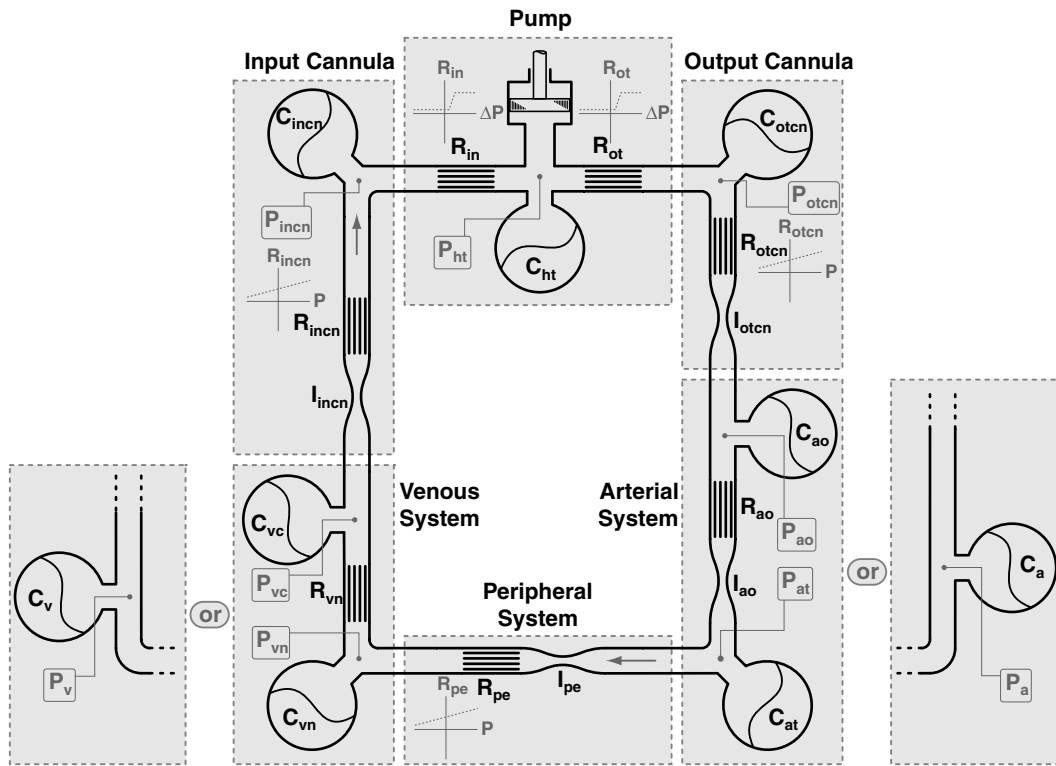


FIGURE 4. The overall circulatory system model.

(see Fig. 4). Various pressures of interest and model parameters are also annotated in Fig. 4.

### SIMULATION RESULTS

One of the major advantages of a lumped parameter model is that segments can be added or removed with relative ease, and with this in mind it is instructive to examine two distinct model configurations. The “linear configuration” uses the basic linear arterial and venous segments, while the “nonlinear configuration” includes both the nonlinear arterial segment and the nonlinear venous segments. A comparison of these two configurations illustrates the differences in pressure and flow waveforms, and the improved dynamic characteristics that the nonlinear segments provide. As well, the simpler linear configuration resembles many of the mock circulatory systems in common use such as the Donovan MCS.<sup>3</sup> To aid comparison of the two configurations, the pump was run in fixed rate mode, with a beat rate of 60 bpm and an ejection duty cycle of 0.3.

The governing equations (included in the Appendices) and supporting constitutive relations Eqs. (5)–(12) can be integrated numerically using software such as Mathematica or MATLAB. Care must be taken to choose appropriate integrating routines (for example, in MATLAB we use ODE23s, a modified Rosenbrock method for solving stiff differential equations).<sup>17</sup> The simulated pressure traces for

the vessel proximal to the pump (i.e., the arterial compliance in the linear configuration and the aortic compliance in the nonlinear configuration) over a three-second interval are shown in Fig. 5.

Both pressure curves are similar to what one might see in the human circulatory system, but the dual-compliance arterial model produces features not seen in the single

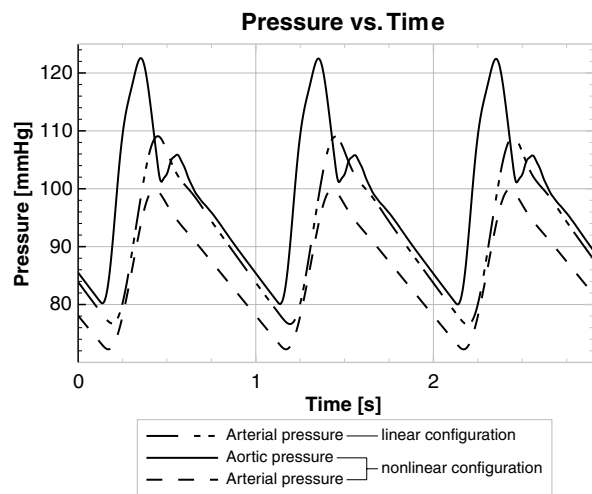


FIGURE 5. A comparison of arterial pressure versus time, as predicted by the arterial SCM and DCM.

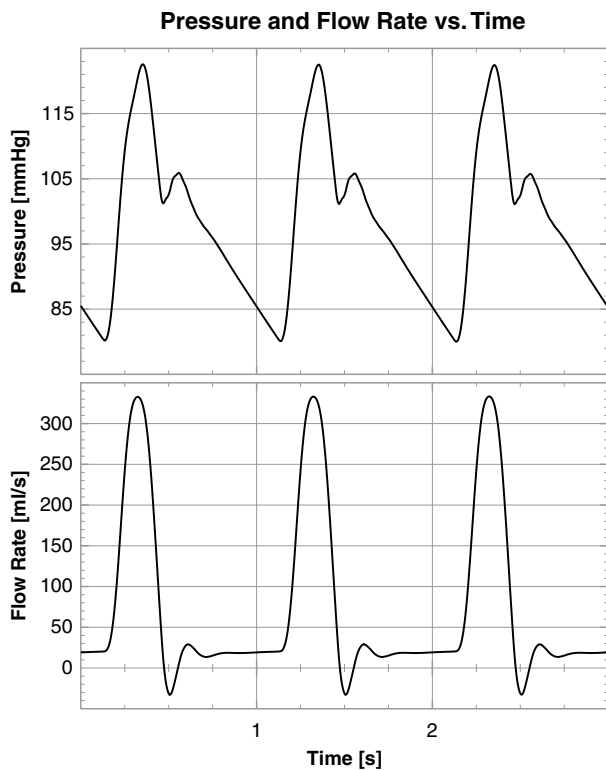


FIGURE 6. Plot of aortic pressure and flow waveforms.

compliance model. Most noteworthy is the appearance of the diastolic notch. Both pressure traces can display a high-frequency oscillatory component, however the cannula flow resistance element quickly damps the high-frequency pressure oscillations so that there is little evidence of them in the figure.

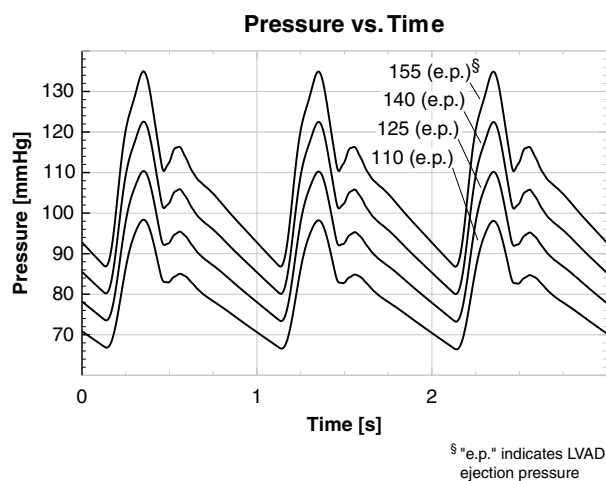


FIGURE 7. A comparison of peripheral flow rate versus time, as predicted by the original<sup>21</sup> and newer<sup>2</sup> circulatory system models.

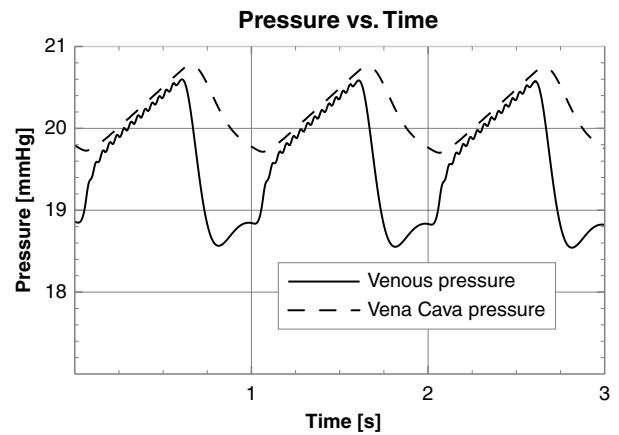


FIGURE 8. A comparison of venous pressure(s) versus time, as predicted by the venous SCM and DCM.

The nonlinear arterial model shows “improved” pressure-volume-flow behaviour (in terms of representing physiological conditions) when compared with the behaviour of the linear model. The pressure wave characteristics can be used to diagnose cardiovascular dysfunction,<sup>13</sup> which suggests these features are important indicators in the human circulatory system. This result is a structural change in the model that is readily investigated in simulation. It would have been an unlikely result of work on most existing MCSs that use a single arterial element (such as<sup>3,15,20,26</sup>) since their design is based on matching the impedance of the HCS<sup>3,4,8,15</sup> rather than direct consideration of system’s internal dynamics.

Figure 6 presents the aortic pressure and flow waveforms over a three-second interval. Note that even though we do not use measured flow data (from *in vivo* experiments) to drive the model, *both* the aortic pressure and flow waveforms agree well with results appearing in the literature.<sup>12,19</sup> In order to demonstrate the robustness of the arterial model, the pumping force input was changed over a range of values. The resultant aortic pressure waveforms are shown in Fig. 7.

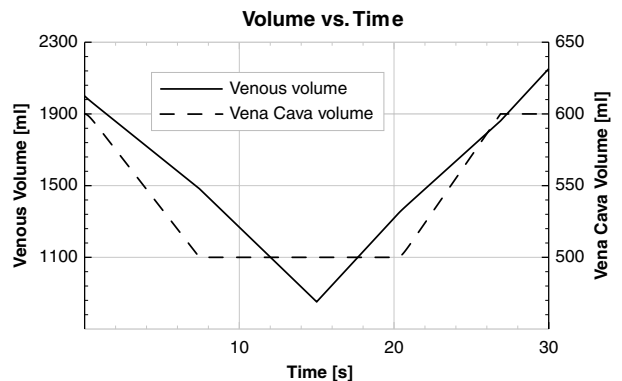


FIGURE 9. Venous volumes under varying inflow and outflow.

An increase in pumping force produces a corresponding increase in mean arterial pressure, as would be expected; the general shape of the pressure waveform remains consistent.

Venous pressures for the nonlinear configuration are shown in Fig. 8. As noted earlier, the systemic venous pressure is adjusted to a higher value than that found in the body, as the venous pressure is solely responsible for filling the pump.

In order to see the low-pressure collapse of the venous model, we need to apply suction to the segment; it is easier to do this by separating the three venous components from the rest of the mock circulatory system. By controlling the flow in-to and out-of the segments, we can easily induce venous collapse and the corresponding increase in flow resistance. This scenario is shown in Fig. 9.

In this simulation, the inflow and outflow into the dual-compliance venous model (whose hydraulic schematic was illustrated in the bottom half of Fig. 3) are varied independently. Between  $t = 0$  s and  $t = 15$  s, the outflow was set higher than the inflow, resulting in a net outflow from the venous system. Initially both the venous and vena cava compliance volumes drop, but the vena cava compliance element quickly reaches its “critical” volume of  $500 \text{ cm}^3$ , and collapses. This collapse is accompanied by a corresponding increase in venous flow resistance.

From time  $t = 15$  s to  $t = 30$  s, the inflow and outflow conditions are reversed, resulting in a net inflow into the venous system. The blood volume in both vessels increases, but the vena cava reaches its nominal volume of  $600 \text{ cm}^3$ , and stiffens. The blood continues to accumulate in the linear veins.

## CONCLUSIONS

Two model configurations are presented for the investigation of the dynamics of the circulatory system and its interaction with ventricular assist devices or total artificial hearts. Both model configurations produce pressure and flow behaviours which are physiologically sound, however the addition of the two nonlinear (arterial and venous) segments makes the nonlinear model much more representative of the human circulatory system. The much-improved arterial behaviour is particularly noteworthy because this result is due to the relative ease with which structural modifications can be made and investigated when using a computer model rather than a physical model such as a mock circulatory system.

There are many mathematical models of the human circulatory system available in the literature, and these vary both in terms of complexity and scope, based on their intended use. Direct comparisons between models are therefore difficult (and are not attempted in this paper, although references to several other models are included). Differences between the various models are owing to their unique design goals. The goal of this model (as outlined above) is to aid LVAD development and mock circulatory loop design

by providing a lumped parameter simulation of the systemic side of the human circulatory system, with each component based on physiological data available in the literature.

All of the parameters for the circulatory system model are based, either directly or indirectly, on published data. Although the present model does not allow study of micro-behaviour in the human circulatory system, the advantages of a lumped parameter configuration (such as the ability to add and remove segments at will, or the ease of simulation) allow for some very interesting studies of the macro-scale circulatory behaviour.

## APPENDIX

### A. STATE EQUATIONS FOR THE MODEL

The following differential equations describe the behaviour of the model with the linear arterial and linear venous segments inserted:

$$\dot{s}_{ht}(t) = \frac{p_{ht}(t)}{I_{ht}} \quad (\text{A.1})$$

$$\dot{p}_{ht}(t) = F(t) - \frac{p_{ht}(t) \cdot R_{ht}}{I_{ht}} - A_{ht} \cdot P_{ht}(V_{ht}(t)) \quad (\text{A.2})$$

$$\begin{aligned} \dot{V}_{ht}(t) = & \frac{p_{ht}(t) \cdot A_{ht}}{I_{ht}} \\ & + R_{inv}(P_{incn}(V_{incn}(t)) - P_{ht}(V_{ht}(t))) \\ & - R_{otv}(P_{ht}(V_{ht}(t)) - P_{otcn}(V_{otcn}(t))) \end{aligned} \quad (\text{A.3})$$

$$\begin{aligned} \dot{V}_{otcn}(t) = & R_{otv}(P_{ht}(V_{ht}(t)) - P_{otcn}(V_{otcn}(t))) \\ & - \frac{p_{otcn}(t)}{I_{otcn}} \end{aligned} \quad (\text{A.4})$$

$$\begin{aligned} \dot{p}_{otcn}(t) = & P_{otcn}(V_{otcn}(t)) - \frac{p_{otcn}(t) \cdot R_{otcn}}{I_{otcn}} \\ & - P_a(V_a(t)) \end{aligned} \quad (\text{A.5})$$

$$\dot{V}_a(t) = \frac{p_{otcn}(t)}{I_{otcn}} - \frac{p_{pe}(t)}{I_{pe}} \quad (\text{A.6})$$

$$\dot{p}_{pe}(t) = P_a(V_a(t)) - \frac{R_{pe} \cdot p_{pe}(t)}{I_{pe}} \quad (\text{A.7})$$

$$\dot{V}_v(t) = \frac{p_{pe}(t)}{I_{pe}} - \frac{p_{incn}(t)}{I_{incn}} \quad (\text{A.8})$$

$$\begin{aligned} \dot{p}_{incn}(t) = & P_v(V_v(t)) - \frac{p_{incn}(t) \cdot R_{incn}}{I_{incn}} \\ & - P_{incn}(V_{incn}(t)) \end{aligned} \quad (\text{A.9})$$

$$\begin{aligned} \dot{V}_{incn}(t) = & \frac{p_{incn}(t)}{I_{incn}} - R_{inv}(P_{incn}(V_{incn}(t))) \\ & - P_{ht}(V_{ht}(t)) \end{aligned} \quad (\text{A.10})$$



```

function o1 = Pao(i1,i2) % PAO - Aortic pressure function
% i2 is 1 for cubic, 2 for exponential, anything else for linear
if i2==1
    o1=7.66e-6*i1^3-0.00175*i1^2+0.151*i1-4.08;
elseif i2==2
    o1=-1.43*log(1.37-0.00943*i1);
else
    o1=i1/29.3-1.94226;
end

function o1 = Pat(i1) % PAT - Arterial pressure function
o1=i1/100.7-4.64431;

function o1 = Pvn(i1) % PVN - Venous pressure function
o1=i1/2500-0.533579;

function o1 = Pvc(i1) % PVC - Vena cava pressure function
if i1<=600
    if i1>=500
        o1=(i1-500)/500;
    else
        o1=(i1-500)*10;
    end
else
    o1=(i1-600)*10-1/5;
end

function o1 = Pincn(i1) % PINCN - Inlet cannula pressure function
o1=i1/1.19-26.2001;

function o1 = Force(i1) % FORCE - Fixed-rate pumping force
if mod(i1,1)<0.35
    o1=37.5;
else
    o1=2.5;
end

% function o1 = Force(i1,i2)
% % FORCE - FFFE pumping force
% %
% global IN_SYSTOLE PREV_T
%
% if(IN_SYSTOLE==0)
%     if((i2>=100)&(PREV_T<i1))
%         IN_SYSTOLE=1;
%         PREV_T=i1;
%         o1=50;
%         %disp('Switched from diastole to systole');
%     else
%         o1=0;
%     end
% else
%     if((i2<=20)&(PREV_T<i1))
%         IN_SYSTOLE=0;
%         PREV_T=i1;
%         o1=0;
%         %disp('Switched from systole to diastole');

```

```

% else
%   o1=50;
% end
% end
function dydt = f(t,y)
% F - State derivatives
%
% 1 - sPiston; 2 - pPiston; 3 - VHeart; 4 - VOutletCannula
% 5 - pOutletCannula; 6 - VAorta; 7 - pAorta; 8 - VArteries
% 9 - pPeripheral; 10 - VVeins; 11 - VVenaCava; 12 - pInletCannula
% 13 - VInletCannula

% Static parameter values (inertias)
Iht=0.025;
Iotcn=5.1e-5;
Iao=3.4e-5;
Ipe=0.0275;
Iincn=3.4e-5;

% Static parameter values (resistances)
Rht=0.25;
Rotcn=0.0011;
Rao=0.0011;
Rpe=0.013;
Rincn=1.3e-5;

% Static parameter values (piston c-sec area)
Aht=19.27;

dydt=zeros(13,1);

dydt(1)=y(2)/Iht;
dydt(2)=Force(t)-y(2)*Rht/Iht-Aht*Pht(y(3));
dydt(3)=y(2)/Iht*Aht+R(Pincn(y(13))-Pht(y(3)))-R(Pht(y(3))- ...
Potcn(y(4)));
dydt(4)=R(Pht(y(3))-Potcn(y(4)))-y(5)/Iotcn;
dydt(5)=Potcn(y(4))-y(5)*Rotcn/Iotcn-Pao(y(6),3);
dydt(6)=y(5)/Iotcn-y(7)/Iao;
dydt(7)=Pao(y(6),3)-y(7)*Rao/Iao-Pat(y(8));
dydt(8)=y(7)/Iao-y(9)/Ipe;
dydt(9)=Pat(y(8))-y(9)*Rpe/Ipe-Pvn(y(10));
dydt(10)=y(9)/Ipe-Rvn(Pvn(y(10))-Pvc(y(11)));
dydt(11)=Rvn(Pvn(y(10))-Pvc(y(11)))-y(12)/Iincn;
dydt(12)=Pvc(y(11))-y(12)*Rincn/Iincn-Pincn(y(13));
dydt(13)=y(12)/Iincn-R(Pincn(y(13))-Pht(y(3)));

```

## ACKNOWLEDGMENTS

The authors wish to acknowledge the financial support of the Natural Sciences and Engineering Research Council of Canada as well as support from the Medical Devices Centre located at the University of Ottawa Heart Institute. We also acknowledge the contributions of Sean Tan and Vinay Menon who contributed to the development of this model during their graduate studies.

## REFERENCES

- <sup>1</sup>Babbs, C. F. Theoretical advantages of abdominal counterpulsation in cpr as demonstrated in a simple electrical model of the circulation. *Ann. Emerg. Med. Part I* 13:660-671, 1984.
- <sup>2</sup>Conlon, M. J. Design and evaluation of a neural network-based controller for an artificial heart. Master's thesis, Carleton University, 2000.
- <sup>3</sup>Donovan, F. H. Design of a hydraulic analog of the human circulatory system for evaluating artificial hearts. *Biomat. Med. Dev. Artif. Org.* 3(4):439-49, 1975.

- <sup>4</sup>Ferrari, G., C. De Lazzari, R. Mimmo, D. Ambrosi, and G. Tosti. Mock circulatory system for *in vitro* reproduction of the left ventricle, the arterial tree and their interaction with a left ventricular assist device. *J. Med. Eng. Technol.* 18(3):87–95, 1994.
- <sup>5</sup>Fung, Y. C. *Biomechanics: Circulation*, 2nd ed. Springer-Verlag, 1994.
- <sup>6</sup>Guyton, A. C. *Human Physiology and Mechanisms of Disease*. 5th ed. W. B. Saunders, 1992.
- <sup>7</sup>King, A. L. Pressure-volume relation for cylindrical tubes with elastomeric walls: The human aorta. *J. Appl. Phys.* 17(6):501–505, 1946.
- <sup>8</sup>Kolff, W. J. Mock circulation to test pumps designed for permanent replacement of damaged hearts. *Clev. Clin. Quart.* 26:223–226, 1959.
- <sup>9</sup>Laskey, W. K., H. G. Parker, V. A. Ferrari, W. G. Mussmaul, and A. Noodergraaf. Estimation of total systemic arterial compliance in humans. *J. Appl. Phys.* 69(1):112–119, 1990.
- <sup>10</sup>Lee, T. C., K. F. Huang, *et al.* Electrical lumped model for arterial vessel beds. *Comput. Met. Prog. Biomed.* 73(3):209–219, 2004.
- <sup>11</sup>Liu, K. P., Z. Brin, and F. C. P. Yin. Estimation of total arterial compliance: An improved method and evaluation of current methods. *Am. J. Physiol.* 251(20):H588–H600, 1986.
- <sup>12</sup>Lu, K. Jr., J. W. Clark, F. H. Ghorbel, D. L. Ware, and A. Bidani. A human cardiopulmonary system model applied to the analysis of the Valsalva maneuver. *Am. J. Physiol. Heart Circ. Physiol.* 281(6):H2661–H2679, 2001.
- <sup>13</sup>McGhee, B. H., and E. J. Bridges. Monitoring arterial blood pressure: What you may not know. *Crit. Care Nurse* 22(2):60–78, 2002.
- <sup>14</sup>Menon, V. Fuzzy logic controller for an artificial heart. Master's thesis, Carleton University, 1998.
- <sup>15</sup>Mrava, G. L. Mock circulation system for artificial hearts. *Adv. Biomed. Eng. Med. Phys.* 3:115–130, 1970.
- <sup>16</sup>Ogino, H., N. Klangasuk, W. Jin, C. T. Bowles, and M. H. Yacoub. Influence of the compliance of the pump housing and cannulas of a paracorporeal pneumatic ventricular assist device on transient pressure characteristics. *Artif. Org.*, 19(6):525–534, 1995.
- <sup>17</sup>Shampine, L. F., and M. W. Reichelt. The MATLAB ODE suite. *SIAM J. Sci. Comput.* 18(1):1–22, 1997.
- <sup>18</sup>Stergiopoulos, N., J. J. Meister, and N. Westerhof. Simple and accurate way for estimating total and segmental arterial compliance: The pulse pressure method. *Ann. Biomed. Eng.* 22(4):392–397, 1994.
- <sup>19</sup>Stergiopoulos, N., B. E. Westerhof, and N. Westerhof. Total arterial compliance as the fourth element of the windkessel model. *Am. J. Physiol.* 276(1):H81–H88, 1999.
- <sup>20</sup>Swanson, W. M., and R. E. Clark. A simple cardiovascular system simulator. *J. Bioeng.* 1(2):135–145, 1977.
- <sup>21</sup>Tan, S. Development of a dynamic model of a ventricular assist device for investigation of control systems. Master's thesis, Carleton University, 1996.
- <sup>22</sup>Tortora, G. J., and S. R. Grabowski. *Principles of Anatomy and Physiology*, 9th ed. John Wiley and Sons, 2000.
- <sup>23</sup>Tsach, U., D. B. Geselowitz, A. Sinha, and H. K. Hsu. A novel output-feedback pusher plate controller for the penn state electric ventricular assist device. *J. Dyn. Syst. Meas. Cont. Trans. ASME* 111(1):69–74, 1989.
- <sup>24</sup>Tsitlik, J. E., and H. R. Halperin, *et al.* Modeling the circulation with three-terminal electrical networks containing special nonlinear capacitors. *Ann. Biomed. Eng.* 20(6):595–616, 1992.
- <sup>25</sup>White, F. M. *Fluid Mechanics*. 3rd ed. McGraw-Hill, 1994.
- <sup>26</sup>Woodruff, S. J., M. K. Sharp, and G. M. Pantalos. Compact compliance chamber design for the study of cardiac performance in microgravity. *ASAIO J.* 43(4):316–320, 1997.
- <sup>27</sup>Xu, L., and M. Fu. Computer modeling of interactions of an electric motor, circulatory system, and rotary blood pump. *ASAIO J.* 46(5):604–611, 2000.